Theor Chem Acc (2002) 108:168–178
DOI 10.1007/s00214-002-0374-6

Theoretical
Chemistry Accounts

Regular article

A variationally stable quasi-relativistic method: low-order approximation to the normalized elimination of the small component using an effective potential

Michael Filatov, Dieter Cremer

Theoretical Chemistry, University of Göteborg, Reutersgatan 2, 41320 Göteborg, Sweden

Received: 1 April 2002 / Accepted: 23 June 2002 / Published online: 30 August 2002

Abstract. A simple and variationally stable quasi-relativistic method based on a modified low-order (LO) approximation to the normalized elimination of the small component (NESC) method is presented. The modification of the original LO-NESC scheme implies the use of an energy-independent factor in the relativistic correction to the potential energy. This factor cuts off the potential energy at short distances from the nucleus and in this way restores the variational stability of LO-NESC. The new method, dubbed LO-NESC-effective potential (EP) was tested in calculations on one-, two- and many-electron atoms. The LO-NESC-EP can be easily implemented into the existing nonrelativistic quantum-chemical program codes because its Hamiltonian matrix can be expressed entirely in terms of the integrals appearing in a nonrelativistic calculation.

Key words: Relativistic theory – Normalized elimination of the small component – Variational stability – Effective potential

1 Introduction

Despite the importance of relativity for the chemistry of heavy elements [1, 2, 3] all-electron relativistic quantum-chemical calculations still remain quite uncommon. Few research groups can afford to do all-electron Dirac–Hartree–Fock (DHF) [4] or post-DHF [5, 6] calculations on larger chemical systems. An obvious reason for this fact is the high computational cost of calculations based on the four-component Dirac formalism. Despite enormous progress in the development of relativistic and quasi-relativistic quantum-chemical methods during the last few decades [6, 7, 8, 9, 10, 11, 12, 13, 14, 15, 16, 17, 18, 19, 20] there is still a need for the development of simple, yet effective, approximate computational schemes for all-electron relativistic calculations.

The major step in such a development is the reduction of the full four-component formalism to a two-component or a one-component form [7]. The various approaches proposed in this connection are the Douglas–Kroll–Hess (DKH) method [8, 9, 10], the zero-order regular approximation (ZORA) [11, 12, 13], the relativistic elimination of the small component (RESC) [14], the normalized elimination of the small component (NESC) [15], etc. Various perturbational approaches which expand the full four-component Dirac Hamiltonian in powers of $1/c^2$ have also been developed [16].

The DKH method relies strongly on the resolution of the identity when calculating the matrix elements of the Hamiltonian and sometimes this method can yield counterintuitive results, for example, lower total energies with smaller basis sets [9]. The ZORA method overestimates the relativistic energy correction for the innermost electrons by almost a factor of 2 [13]. Furthermore, it is difficult and so far an unsolved problem to represent the matrix elements of the ZORA Hamiltonian in analytic form [13, 17]. The RESC method is variationally unstable in the sense that the tight basis functions needed to describe the correct behavior of the relativistic wavefunction near the atomic nucleus lead to a variational collapse [18].

The NESC approach [15] is free of such drawbacks; however, it is still computationally demanding because it employs an energy-dependent relativistic metric which makes a four-index transformation of the electron-repulsion integrals mandatory for each self-consistent cycle [15]. A low-order (LO) approximation [19] (correct to order $1/c^2$) to NESC avoids using the energy-dependent metric. Such an approximation is free of the pathologically divergent operators appearing in the Breit–Pauli quasi-relativistic Hamiltonian and might be expected to be stable in variational calculations [19]. Nevertheless, the originally proposed LO-NESC (dubbed NESC $\mathbf{U} = \mathbf{I}$ [19]) method failed to be stable in actual variational calculations on atomic and molecular systems and was abandoned despite its appealing features [19].

Correspondence to: D. Cremer
e-mail: dieter.cremer@theoc.gu.se

Beside the aforementioned difficulties, all the quasi-relativistic approaches currently available suffer from the fact that they are not well suited for implementation within existing nonrelativistic quantum-chemical computer codes. For example, (quasi-)relativistic methods require the calculation of molecular integrals not needed for a nonrelativistic quantum-chemical calculation. The lack of highly efficient algorithms easy to implement in nonrelativistic computer programs still hinders the application of relativistic quantum-chemical approaches on a larger scale.

It is a primary goal of the current work to set up a computationally efficient quasi-relativistic method which can be easily incorporated into existing quantum-chemical programs without changing larger parts of the original software. In this respect, it seems tempting to revisit the LO-NESC. This approximate scheme possesses highly attractive features when including relativistic effects into nonrelativistic methods, in particular as unusual molecular integrals are not needed when calculating the Hamiltonian matrix elements of the LO-NESC approach. The major problem of the LO-NESC method is its variational instability in the sense that its Hamiltonian is not bounded from below. It is demonstrated in Sect. 2 that with a slight modification of the original approximate scheme the variational stability is restored. For this purpose the relativistic correction is modified by the use of an effective (energy-independent) potential-energy function depending on a cutoff factor. This factor regularizes the relativistic correction to the nuclear–electron attraction in the close vicinity of the nucleus, thus taking care of the fact that in this region the exact nuclear–electron attraction is considerably weaker than can be expressed with an approximate linear operator. In the current work, the cutoff factor was parameterized utilizing results of the four-component relativistic calculations of hydrogen-like atomic ions. Benchmark calculations on atomic and molecular systems performed with the proposed method are compared with available literature data in Sect. 3.

2 Theory

2.1 Method

Solution of the Dirac equation (Eqs. 1, 2),

$$(V-E)\Psi_{\mathrm{L}} + c(\sigma\cdot\mathbf{p})\Psi_{\mathrm{S}} = 0 \ , \tag{1}$$

$$c(\sigma\cdot\mathbf{p})\Psi_{\mathrm{L}} + (V-E-2mc^2)\Psi_{\mathrm{S}} = 0 \ , \tag{2}$$

leads to the four-component Dirac wavefunction [20] $\Psi_{\mathrm{D}} = \begin{pmatrix}\Psi_{\mathrm{L}}\\ \Psi_{\mathrm{S}}\end{pmatrix}$, where Ψ_{L} is the large and Ψ_{S} the small component of the Dirac wavefunction, V is the potential, σ is the vector of the Pauli matrices [21], $\sigma = (\sigma_{\mathrm{x}}, \sigma_{\mathrm{y}}, \sigma_{\mathrm{z}})$, $\mathbf{p} = -i\hbar\nabla$ is the momentum operator, c is the velocity of light, and m is the electron mass.

The NESC method of Dyall [15, 19, 22] is based on the replacement of the small component, Ψ_{S}, in Eqs. (1, 2) by the pseudolarge component [22], Φ_{L}:

$$\Psi_{\mathrm{S}} = \frac{(\sigma\cdot\mathbf{p})}{2mc}\Phi_{\mathrm{L}}. \tag{3}$$

With the help of Eq. (3) the Dirac equation (Eqs. 1, 2) is modified to Eqs. (4) and (5),

$$\hat{T}\Phi_{\mathrm{L}} + V\Psi_{\mathrm{L}} = E\Psi_{\mathrm{L}} \ , \tag{4}$$

$$\hat{T}\Psi_{\mathrm{L}} + \frac{1}{4m^2c^2}(\sigma\cdot\mathbf{p})(V-E)(\sigma\cdot\mathbf{p})\Phi_{\mathrm{L}} = \hat{T}\Phi_{\mathrm{L}} \ , \tag{5}$$

where $\hat{T}$ is the kinetic energy operator,

$$\hat{T} = \frac{\mathbf{p}^2}{2m} = \frac{(\sigma\cdot\mathbf{p})(\sigma\cdot\mathbf{p})}{2m} \ . \tag{6}$$

The elimination of Φ_{L} from Eqs. (4, 5) is accomplished [15] with the help of Eq. (7),

$$\Phi_{\mathrm{L}} = \hat{U}\Psi_{\mathrm{L}} \ , \tag{7}$$

which connects the large and the pseudolarge components of the modified four-component wavefunction with the help of a nonunitary operator, $\hat{U}$. On premultiplying Eq. (5) by $\hat{U}^{\dagger}$, replacing Φ_{L} according to Eq. (7), and adding to Eq. (4), one gets Eq. (8), which depends on the large component only [15]:

$$\left[\hat{T} - (\hat{I}-\hat{U}^{\dagger})\hat{T}(\hat{I}-\hat{U}) + V + \frac{1}{4m^2c^2}\hat{U}^{\dagger}(\sigma\cdot\mathbf{p})V(\sigma\cdot\mathbf{p})\hat{U}\right]\Psi_{\mathrm{L}}$$
$$= E\left(1+\frac{\hat{U}^{\dagger}\hat{T}\hat{U}}{2mc^2}\right)\Psi_{\mathrm{L}}. \tag{8}$$

In Ref. [15], the nonunitary energy-dependent operator, $\hat{U}$ of Eqs. (7) and (8) is expressed in a matrix form suitable for finite-basis calculations. It possesses the property expressed in Eq. (9):

$$\hat{U} = \hat{I} + o(1/c^2) \, , \tag{9}$$

where $\hat{I}$ is the identity operator.

As follows from Eqs. (1), (2), and (3), the components of the modified Dirac wavefunction satisfy Eq. (10) [22],

$$(\sigma\cdot\mathbf{p})\Psi_{\mathrm{L}} = \left(1+\frac{E-V}{2mc^2}\right)^{-1}(\sigma\cdot\mathbf{p})\Psi_{\mathrm{L}} \, , \tag{10}$$

which is analogous to the relation connecting the large and small components of the original Dirac wavefunction.

The NESC master equation (Eq. 8) is equivalent to the Dirac equation projected onto the set of positive energy states [15]; thus, there is no danger of obtaining the negative energies $E < -2mc^2$ from Eq. (8). For brevity, the subscript L, which labels the large component, is dropped in the following.

The major drawback of Eq. (8) is the dependence of the operator $\hat{U}$ on the energy eigenvalues. However, the property (Eq. 9) of the operator $\hat{U}$ enables one to define [19] a LO approximation to Eq. (8) defining the NESC method. Thus, by setting $\hat{U} = \hat{I}$ one gets Eq. (11) from Eq. (8); Eq. (11) is correct to the order of $1/c^2$ and no longer contains energy-dependent operators [19]:

$$\left[\hat{T} + V + \frac{1}{4m^2c^2}(\sigma\cdot\mathbf{p})V(\sigma\cdot\mathbf{p})\right]\Psi = E\left(1+\frac{\hat{T}}{2mc^2}\right)\Psi \ . \tag{11}$$

Equation (11) contains LO relativistic corrections to both the Hamiltonian operator and the metric of Ψ. As has been shown [19], the relativistic metric of Eq. (11) helps to avoid the pathological mass-velocity and Darwin terms of the Pauli approximation; hence, Eq. (11) can be used in a quasi-variational calculation [19], while any approach based on the Pauli Hamiltonian requires the use of perturbation theory. However, the actual stability of Eq. (11) in variational calculations depends on the potential, V. For the potential $V = -Z/r$ of a point nucleus, the third term in parentheses on the left-hand side (lhs) of Eq. (11) diverges as $-Z/r^3$ at short distances from the nucleus and prevails over the kinetic energy term. Even the use of the potential of a finite nucleus (with nuclear radius obtained from experimental data) does not help to overcome the problem [19]. When calculating hydrogen-like atomic ions with Eq. (11) and a single s-type Gaussian trial wavefunction, the optimal value of the Gaussian exponent was obtained to be infinite [19]. According to Dyall [19] the kinetic energy and the potential energy are disbalanced and this is suspected to be responsible for the variational collapse of the LO-NESC approximation (see also the Appendix).

Closer inspection of Eq. (8), however, suggests that the total kinetic energy will not increase if one employs the exact energy-dependent operator $\hat{U}$ instead of the approximation $\hat{U} = \hat{I}$. What actually happens in such a case is a decrease in the total potential energy. Let us assume that the exact solution, Ψ, of Eq. (8) is known. With the help of Eqs. (6) and (10) and the hermiticity of the operator $\sigma\cdot\mathbf{p}$, Eq. (8) can be rewritten in the form of Eq. (12),

$$(\hat{T} + V)\Psi + \frac{1}{4m^2c^2}(\sigma\cdot\mathbf{p}) \times \left[Vw^2 - 2mc^2(1-w)^2 + E(1-w^2)\right](\sigma\cdot\mathbf{p})\Psi = E\left(1 + \frac{\hat{T}}{2mc^2}\right)\Psi\,, \qquad (12)$$

which is similar in its appearance to Eq. (11). In Eq. (12), w denotes the prefactor on the right-hand side (rhs) of Eq. (8): $w = [1 + (E-\mathrm{V})/(2mc^2)]^{-1}$. The term in brackets in Eq. (12) can be considered as an effective (energy-dependent) potential (EP), V_{eff}, which after little algebra is given by Eq. (13):

$$V_{\mathrm{eff}} = Vw + E(1-w) = \frac{V + E\frac{(E-V)}{2mc^2}}{1 + \frac{(E-V)}{2mc^2}}\,. \qquad (13)$$

Despite the similarity between Eqs. (11) and (12), the latter is exact and contains beside LO also high-order relativistic corrections hidden in the EP (Eq. 13).

Using for E the Dirac eigenenergy for the $1s_{1/2}$ orbital, $E_{1s_{1/2}} = c^2\left(\sqrt{1 - Z^2/c^2} - 1\right)$, a simple numeric analysis of Eq. (13) reveals the following:

1. At large distances from the nucleus, V_{eff} is virtually identical to the Coulomb potential $-Z/r$.
2. At short distances from the nucleus, V_{eff} is considerably less negative than $-Z/r$ and possesses a cusp rather than a singularity at the nucleus.
3. V_{eff} starts to deviate markedly from $-Z/r$ already at distances of the order of $Z/(mc^2)$ [Z times the Thomson radius of the electron, $r_{\mathrm{T}} = 1/(mc^2)$].

This is illustrated in Fig. 1 for $Z = 96$ (the highest atomic number used in test calculations with the LO-NESC in Ref. [19]).

These findings help to understand why the use of potential V even for a nucleus with finite size possessing the experimentally determined radius does not prevent variational collapse of the LO-NESC [19]. The experimental nuclear radii are several orders of magnitude shorter [23] than the Thomson radius of the electron. Figure 1 illustrates that the LO-NESC with $\hat{U} = \hat{I}$ breaks down at distances shorter than $Z/(mc^2)$. At such distances the potential V in Eq. (8) cannot be considered to be weak and the full energy-dependent operator $\hat{U}$ must be used to regularize the singular Coulomb potential.

However, Eqs. (12) and (13) suggest a simple remedy for the variational collapse of Eq. (11). It should be possible to restore the variational stability of the LO-NESC by using a potential V', which is regular close to the nucleus, in the third term on the lhs of Eq. (11). Such a potential, like V_{eff} in Eq. (12), will introduce higher-order relativistic corrections into Eq. (11), albeit in an implicit manner. A reasonable choice for such an EP is the potential of a finite nucleus with an effective "radius" of approximately $Z/(mc^2)$ (see Appendix). Among the various potentials currently in use, the potential of the Gaussian charge distribution, $\rho_{\mathrm{G}} = Zr_0^{-3}\pi^{-3/2}\exp(-r^2/r_0^2)$ seems to be the most appealing, owing to the simplicity of its implementation within existing quantum-chemical computer codes [23]. According to Eq. (14), the EP can be factorized into the potential of a

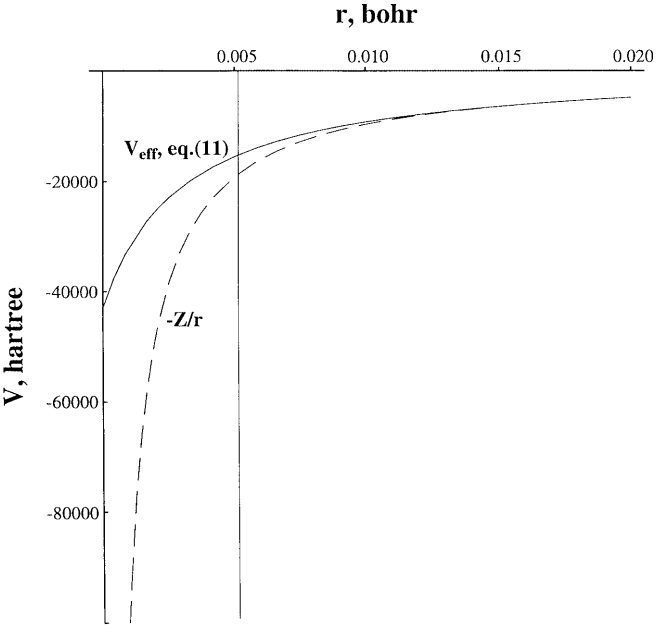

Fig. 1. Comparison of the effective potential from Eq. (13) with the Coulomb potential for $Z = 96$ (see text for details). The *straight vertical line* indicates the position of the cutoff radius, $r_0 = Z/(mc^2)$ for $Z = 96$

point-charge nucleus and the energy-independent cutoff factor:

$$V'(\mathbf{r}) = -\frac{Zn}{r}\mathrm{erf}(r/r_0)\ . \tag{14}$$

The cutoff radius, r_0, in the error function is of the order of the Thomson radius, i.e., $Z/(mc^2)$. Equation (14) eliminates the excess in nuclear–electron attraction close to the nucleus and, therefore, we propose its use in the third term on the lhs of Eq. (11).

In many-electron Hartree–Fock (HF) calculations the total potential, V, consists of the nuclear–electron attraction potential, V_{ne}, and the electron–electron interaction potential, V_{ee}. Thus, in the final form, the proposed one-electron equations take the form of Eq. (15):

$$\left[\hat{T}+V_{\mathrm{ne}}+V_{\mathrm{ee}}+\frac{1}{4m^2c^2}(\sigma\cdot\mathbf{p})V'_{\mathrm{ne}}(\sigma\cdot\mathbf{p})+\frac{1}{4m^2c^2}(\sigma\cdot\mathbf{p})V_{\mathrm{ee}}(\sigma\cdot\mathbf{p})\right]\phi_i$$
$$=\varepsilon_i\left(1+\frac{\hat{T}}{2mc^2}\right)\phi_i. \tag{15}$$

In Eq. (15), ϕ_i is the one-electron, two-component orbital (spinor), and ε_i is the corresponding eigenvalue. The orbitals ϕ_i are normalized by Eq. (16):

$$\left\langle \phi_j\middle|1+\frac{\hat{T}}{2mc^2}\middle|\phi_i\right\rangle = \delta_{ij}\ . \tag{16}$$

The modified nuclear-electron attraction potential, V'_{ne}, in the fourth term on the lhs of Eq. (14) is calculated by Eq. (17),

$$V'_{\mathrm{ne}}(\mathbf{r}_1) = \sum_n^{\mathrm{all}\ n} -\frac{Z_n}{r_{1n}}\mathrm{erf}[r_{1n}/r_0(Z_n)]\ , \tag{17}$$

where $r_0(Z_n)$ is a cutoff radius specific for the nth nucleus and $r_{1\mathrm{n}} = |\mathbf{r}_1-\mathbf{r}_n|$ is the distance between the nth nucleus and the electron position given by radius vector r_1.

The total HF energy is then given by Eq. (18),

$$E_{\mathrm{tot}} = \sum_i^{\mathrm{occ}}\langle\phi_i|\hat{T}+V_{\mathrm{ne}}|\phi_i\rangle + \frac{1}{4m^2c^2}\sum_i^{\mathrm{occ}}\langle\phi_i|(\sigma\cdot\mathbf{p})V'_{\mathrm{ne}}(\sigma\cdot\mathbf{p})|\phi_i\rangle + E_{\mathrm{ee}}, \tag{18}$$

where E_{ee} is the HF electron–electron interaction energy. The HF E_{ee} and V_{ee} are calculated in the usual way but with the electron-repulsion integrals $(\mu\nu|\lambda\tau)$ given in Eq. (12) of Ref. [19]. It is obvious that Eq. (115) may be obtained from Eq. (18) by variation of E with respect to orbitals ϕ_i under the orthonormality constraint (Eq. 16).

2.2 Variational stability, boundedness from below, and gauge invariance

The problem of the variational stability of Eq. (15) is studied along the same lines as in Refs. [12, 19]. First, the dependence of the expectation value of the energy calculated with a single s-type Gaussian trial wavefunction on an exponential parameter, α, is examined for a one-electron atom with $Z = 96$. The results obtained with Eq. (15), the Dirac equation (Eqs. 1, 2), the Schrödinger equation, and with the NESC $\mathbf{U}=\mathbf{I}$ method [19] are presented in Fig. 2. In connection with Eq. (15), the cutoff radius r_0 in the EP (Eq. 17) was chosen to be

$$r_0(Z) = \frac{Z}{mc^2}\ . \tag{19}$$

A comparison of the NESC $\mathbf{U}=\mathbf{I}$ curve with that obtained from Eq. (15) reveals that the use of a modified potential in the fourth term on the lhs of Eq. (15) helps indeed to restore the variational stability. The curve based on Eq. (15) has a single minimum and as the exponential parameter α increases to infinity the energy increases to a large positive constant with limiting value $2mc^2(1-\pi^{-1/2})$.

Equation (15) is bounded from below for a hydrogen-like potential even when using a singular trial wavefunction of the form

$$\psi = Nr^{-a}\exp(-\zeta r),\quad a>0\ . \tag{20}$$

A lower bound for the energy (Eq. 18) does exist provided the cutoff radius r_0 satisfies Eq. (A6) derived in the Appendix. The condition expressed by Eq. (A6) will be violated if the potential in Eq. (17) in the relativistic correction to the Hamiltonian belongs to a finite nucleus with the effective radius r_0 determined from experimental data. This explains why the variational collapse occurs in numeric simulations with the original LO-NESC method [19]. By using Eq. (19) for the actual choice of the cutoff radius, the condition in Eq. (A6) is satisfied and the energy possesses a lower bound for any finite nuclear charge, Z.

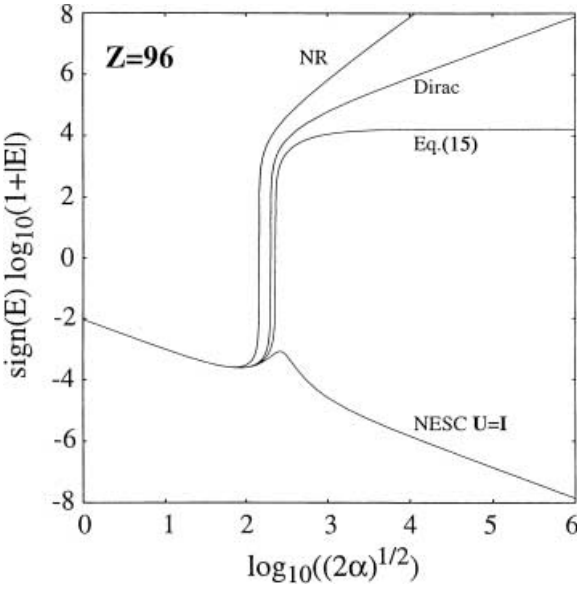

Fig. 2. Energy (in hartree) from Eq. (15), normalized elimination of the small component (NESC $\mathbf{U}=\mathbf{I}$), nonrelativistic (*NR*), and Dirac one-particle equations with a point nucleus and a single Gaussian trial wavefunction (see text for details)

Before turning to the numeric performance of Eq. (15), a comment on its gauge invariance is appropriate. The gauge invariance requires that when the potential in one-electron equations is shifted by a constant value, the orbital energies must automatically be shifted by the same value. An inspection of Eq. (15) suggests that the use of different potentials, V_{ne} and V'_{ne}, may result in breaking the gauge invariance. This does not concern the trivial situation when both V_{ne} and V'_{ne} are shifted by the same constant Δ. In such a case ε_i will be shifted by precisely the same value. A more serious situation will arise if two nuclei k and l approach each other closely. Then, for nucleus k the tail of the potential of nucleus l may approximately be considered as a constant shift of the potential of nucleus k. Since V_{ne} and V'_{ne} are different, both potentials will be shifted differently at nucleus k, namely by $\Delta_{ne} \sim -Z_l/r_{kl}$ and $\Delta'_{ne} \sim -Z_l/r_{kl}\mathrm{erf}[-r_{kl}/r_0(Z_l)]$, respectively. This will result in the shift in the orbital energy being different from both Δ_{ne} and Δ'_{ne}. In principle, this may lead to serious problems when describing chemical bonding [13]. However, beyond a short distance r_0 from a given nucleus both potentials V_{ne} and V'_{ne} become identical. The cutoff radius r_0 in the error function of Eq. (17) is about 3 orders of magnitude shorter ($r_0 \sim 10^{-3}$ bohr) than the length of normal chemical bonds. Thus, given that $r_{kl} \gg r_0(Z_l)$ both shifts, Δ_{ne} and Δ'_{ne} will be identical. Consequently, the orbital energy shift will be the same as Δ_{ne} as is obvious from Eq. (15). This shows that in chemically relevant situations Eq. (15) should not experience any problems with gauge invariance.

3 Results

The performance of the proposed method was tested in calculations on one-, two-, and many-electron atoms. First, calculations for hydrogen-like atomic ions were carried out to obtain a numerically accurate estimate for the eigenvalues and eigenvectors of Eq. (15). These calculations employed a basis set of 62 s-type Gaussian functions with exponential parameters $\alpha_i = Z^2\alpha'_i$, where $\alpha'_i = 8\times10^{-8}$, 1×10^{-7}, 2×10^{-7}, 4×10^{-7},..., 8×10^{7}, 1×10^{8} [9]. Further extension of this basis set even for an atomic ion with $Z = 100$ changes the total energy of the $1s_{1/2}$ state by about 10^{-6} hartree; hence, the eigenvalues obtained can be considered as sufficiently accurate and can be compared with the exact eigenvalues of the Dirac equation.

The relativistic energy corrections $\Delta E_{rel} = E_{rel} - E_{nonrel}$ calculated for the $1s_{1/2}$ states of hydrogen-like atomic ions with Z up to 100 are compared in Fig. 3 with the exact values obtained analytically from the Dirac equation. Some of these data are given in numeric form in Table 1. The Pauli approximation (which employs the nonrelativistic wavefunction) and ZORA are used for comparison. For the ZORA method, which is becoming currently very popular in quasi-relativistic calculations on chemical systems [24], the exact analytic expression for the energy of a hydrogen-like atomic ion is available from the literature [12], while for the Pauli approximation the energy can be calculated directly with the use of the nonrelativistic wavefunction.

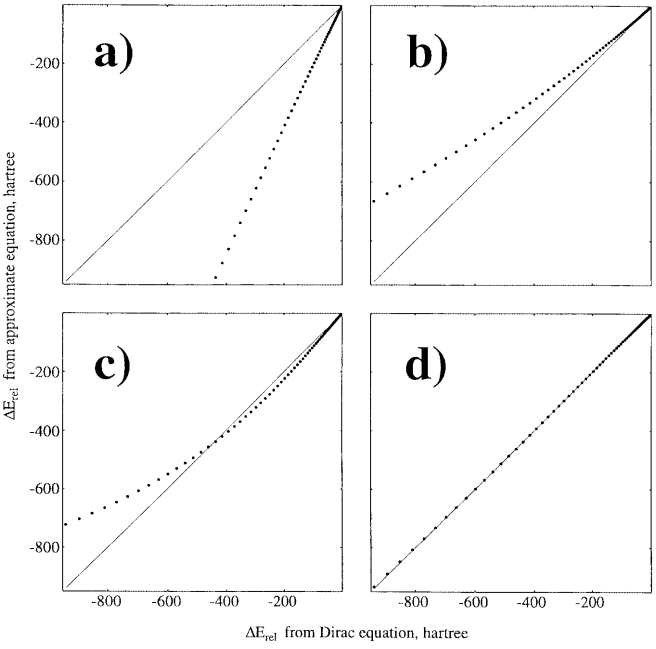

Fig. 3. Relativistic energy correction, ΔE_{rel}, from the Dirac one-particle equation (*solid line*) versus energies from **a** the zero-order regular approximation, **b** the Pauli approximation, **c** Eq. (15) with r_0 from Eq. (19), and **d** Eq. (15) with r_0 from Eq. (21) for hydrogen-like atomic ions (see text for details)

Table 1. Relativistic energy corrections $\Delta E_{rel} = E_{rel} - E_{nonrel}$ (hartree) calculated for hydrogen-like atomic ions. Zero-order regular approximation (*ZORA*)

Z	Dirac[a]	This work[b]	This work[c]	ZORA[d]	Pauli[e]
1	−0.000007	−0.000007	−0.000007	−0.000013	−0.000007
2	−0.000107	−0.000106	−0.000106	−0.000213	−0.000107
10	−0.066742	−0.067209	−0.066658	−0.133573	−0.066565
18	−0.704858	−0.720737	−0.703330	−1.412783	−0.698774
30	−5.524907	−5.869657	−5.509816	−11.117647	−5.391777
50	−44.626156	−51.035381	−44.529248	−90.845507	−41.603215
80	−332.192151	−352.886460	−332.556077	−698.869184	−272.650833
100	−939.195384	−722.200147	−933.502135	−2054.808363	−665.651443

[a] Dirac equation [21]
[b] Equation (15) with r_0 from Eq. (19)
[c] Eq. (15) with r_0 from Eq. (21)
[d] ZORA energies calculated with formulae from Ref. [12]
[e] Energies in the Pauli approximation calculated with the nonrelativistic wavefunctions

The data in Fig. 3 show that the ZORA systematically overestimates (yields too negative) relativistic corrections to the energy, while the Pauli approximation systematically underestimates them. Equation (15) with r_0 from Eq. (19) yields energies either above or below the Dirac reference values. The relativistic energy correction from Eq. (15) is overestimated for lower atomic numbers and underestimated for higher atomic numbers. An obvious reason for the discrepancy is that the shape of EP (Eq. 17) does not match the shape of the potential in Eq. (13) for all atomic numbers. A simple way of circumventing the problem is to parameterize the cutoff radius with the help of the $1s_{1/2}$ eigenvalues of the Dirac equation for hydrogen-like atomic ions. Such a procedure is well defined because a large number of reference data are available. The regularity of the deviation of the calculated energies from the reference values suggests that a simple polynomial dependence of r_0 on Z should be sufficient. By employing only the three parameters a_0, a_1, and a_2 in Eq. (21),

$$r_0(Z)=\left(a_0+a_1Z^{-1}+a_2Z^{-2}\right)\frac{Z}{mc^2}, \qquad a_0=-0.263188, a_1=106.016974, a_2=138.985999, \tag{21}$$

the agreement with Dirac energies is considerably improved for the whole range of nuclear charges ($Z=1-100$). This is exemplified in the fourth column of Table 1 and in Fig. 3d. Equation (15) without fitting of the cutoff radius describes the relativistic corrections, ΔE_{rel}, for hydrogen-like atomic ions ($Z=1-100$) with an average relative error of 8.8%, which has to be compared to 133.3% for ZORA and 9.5% for the Pauli approximation. The use of Eq. (21) reduces the error to 0.2% (standard deviation: 0.13%).

When using Eq. (21), care has to be taken so that the cutoff radius does not fall below the limit imposed in Eq. (A6). Thus, for $Z \geq 132$ the prefactor in Eq. (21) should be set to a constant, which complies with Eq. (A6). A parameterization of r_0 with respect to Z helps to avoid the use of complicated operators in the quasi-relativistic Hamiltonian without losing accuracy. It serves well the actual objective of this work, namely to establish a quasi-relativistic approach for the investigation of large molecules. Hence, Eq. (21) is used in connection with Eq. (15) in all following calculations.

In the case of many-electron atoms, the calculations with Eq. (15) were done first for Helium-like ions up to $Z=100$. The same basis set containing 62 s-type Gaussian functions was employed. The results in Table 2 indicate a reasonable performance of the proposed method for the ground states of two-electron ions. It has to be noted that the reference data from the literature [25, 26, 27] were obtained by employing the potential of a finite nucleus. Usually, calculations with a point-charge nucleus yield lower energies than with a finite-size nucleus (e.g. by about 8 hartree for hydrogen-like uranium) [23].

The straightforward use of Eq. (15) in calculations on many-electron systems may not result in a considerable mitigation of computational effort. One still has to compute a large multitude of additional electron-repulsion integrals when calculating V_{ee} [15, 19]. Such calculations can be as tedious as the four-index transformation of electron-repulsion integrals with the energy-dependent operator $\hat{U}$, which is avoided in Eq. (15). Thus, to benefit from the advantages of Eq. (15) one needs to simplify the calculation of the electron repulsion term.

An obvious simplification results from a renormalization of the one-electron part, $\mathbf{H}_1$, of the quasi-relativistic Hamiltonian in Eq. (15) on the nonrelativistic metric and the use of the so-obtained one-electron quasi-relativistic Hamiltonian, $\mathbf{H'}_1$, within the standard non-relativistic HF approach. As the quasi-relativistic metric in Eq. (15) is energy-independent, the renormalization can be done before the self-consistent-field procedure at negligible computational expense.

$$\mathbf{H'}_1 = \left(\mathbf{S}^{1/2}\right)^{\dagger}\left(\mathbf{X}^{-1/2}\right)^{\dagger}\mathbf{H}_1\left(\mathbf{X}^{-1/2}\right)\left(\mathbf{S}^{1/2}\right), \tag{22}$$

$$X_{\mu\nu} = \left\langle \chi_\mu \middle| 1+\frac{\hat{T}}{2mc^2} \middle| \chi_\nu \right\rangle, \tag{23}$$

$$(H_1)_{\mu\nu} = \left\langle \chi_\mu \middle| \hat{T} + V_{\mathrm{ne}} + \frac{1}{4m^2c^2}(\sigma\cdot\mathbf{p})V'_{\mathrm{ne}}(\sigma\cdot\mathbf{p}) \middle| \chi_\nu \right\rangle. \tag{24}$$

In Eqs. (22), (23), and (24), which give the renormalization of the one-electron part of the Hamiltonian in matrix form, χ_ν are the basis functions used to expand the one-electron orbitals and $\mathbf{S}$ is the matrix of the overlap integrals. It is worth noting that the matrix elements $(H_1)_{\mu\nu}$ can be expressed entirely in terms of the

Table 2. Energies of helium-like atomic ions (hartree). Dirac–Hartree–Fock (*DHF*), variational DHF (*VDHF*)

Z	This work Eq. (15)[a]	This work Eqs. (22), (23), (24)[a]	VDHF[b]	DHF[c]	DHF[d]
2	−2.861813	−2.861795	−2.861813	−2.861812	
10	−93.982590	−93.979233	−93.982799	−93.982695	−93.979479
18	−314.196764	−314.175955	−314.200163		
30	−892.038906	−891.935363		−892.065286	−892.051699
50	−2,556.179995	−2,555.620945		−2,556.310106	−2,556.278645
80	−7,005.996649	−7,002.618418			−7,002.382844
100	−11,780.427281	−11,770.216583			−11,763.908443

[a] Present work, r_0 from Eq. (21)
[b] From Ref. [25]
[c] 14s10p8d7f6g5h4i basis set of G spinors [26]
[d] Basis set of B splines [27]

molecular integrals employed in the nonrelativistic HF calculation [23].

The results of the calculations on helium-like atomic ions utilizing Eqs. (22), (23), and (24) are presented in the third column of Table 2. Such calculations are a stringent test of the performance of Eqs. (22), (23), and (24) because the relativistic correction to the electron-repulsion energy is largest for 1*s* electrons and any inefficient approximation will have a dramatic effect on it. As Table 2 exemplifies, the use of Eqs. (22), (23), and (24) leads to an acceptably small shift in the total energy, for example, 0.08% (about 10 hartree) for $Z = 100$. Thus, the renormalization on the nonrelativistic metric which is also used in some other quasi-relativistic schemes [9, 14] has a small effect on the total energy. However, if one needs properties other than energy, the one-electron orbitals obtained with Eqs. (22), (23), and (24) must be renormalized back to the quasi-relativistic normalization (Eq. 16).

The calculation of the Ag and Au atoms in their ^{2}S ground states is a standard test used when assessing the reliability of approximate relativistic schemes [9, 10, 14, 17, 18]. For these atoms, the results of numeric DHF calculations are available [28] along with the results of DHF calculations using basis sets [14]. In the calculations of these atoms, Eqs. (22), (23), and (24) in connection with the scalar relativistic approximation [9, 10, 14, 20] were used. This approximation implies the elimination of all spin-dependent relativistic corrections with the help of the Dirac relation (Eq. 25):

$$(\sigma \cdot \mathbf{a})(\sigma \cdot \mathbf{b}) = \mathbf{a} \cdot \mathbf{b} + i\sigma \cdot (\mathbf{a} \times \mathbf{b}). \tag{25}$$

For the two atoms Ag and Au, spin–orbit coupling was neglected because it plays a minor role in these cases and its neglect simplifies the calculations. We note however that spin–orbit coupling can be included into Eqs. (22), (23), and (24) because there is no danger of a variational collapse.

The calculations on Ag and Au employed the fully uncontracted (17s12p8d) and (19s14p10d5f) basis sets of Gropen [29]. The results of quasi-relativistic HF calculations based on Eqs. (22), (23), and (24) are compared with the available data from DHF [14, 28] and DKH [9, 10] calculations in Table 3. It has to be noted that the DHF calculations employed the potential of a finite nucleus, whereas the calculations using Eqs. (22), (23), and (24) were done with the point nucleus. Nevertheless, the total atomic energies obtained with Eqs. (22), (23), and (24) are in reasonable agreement with the DHF results.

For the Au atom, Eqs. (22), (23), and (24) yield a somewhat lower total energy than either the numeric DHF or the finite-basis DHF results. This discrepancy has nothing to do with the variational collapse. Thus, an extension of the basis set for Au with eight tight s-type functions in an even-tempered sequence with a ratio of 2.5 results in an energy lowering of just 0.02 hartree. Overestimation of the total energy of Au is probably due to the too low energies of the *ns* orbitals for $n \geq 2$ (Table 3). For the 2*s* orbital of Au, the energy from Eqs. (22), (23), and (24) is 13 hartree lower than from the numeric DHF calculation. This is too much for an orbital energy lowering owing to the use of a point nucleus [23]. Most likely, it is the shape of the EP (Eq. 17) which is responsible for the 2*s* orbital energy. This potential seems to be too "broad" compared to the exact potential (Eq. 13). The EP was fitted via the cutoff radius (Eq. 21) to reproduce the energies of the 1*s* orbitals, whereas this fit procedure may be less precise for higher orbitals.

It is quite unlikely that such an overestimation may affect the energies of the valence electrons. Indeed, the orbital energies of the valence electrons of both Ag and

Table 3. Relativistic orbital energies (hartree) for Ag(^{2}S) and Au(^{2}S). Douglas–Kroll–Hess (*DKH*)

Orbital	Ag			Au		
	This work	DKH[a]	DHF[b]	This work	DKH[a]	DHF[b]
1*s*	−942.4406	−941.9533	−943.1578	−2,980.2372	−2,975.8754	−2,986.1300
2*s*	−142.2593	−141.8774	−141.9930	−545.6464	−531.5596	−532.1880
3*s*	−27.4193	−27.6373	−27.3849	−131.9093	−128.0912	−128.0890
4*s*	−4.2507	−4.2721	−4.2746	−30.0701	−29.1120	−29.1399
5*s*	−0.2247	−0.2372	−0.2814	−4.8008	−4.6965	−4.6845
6*s*				−0.2780	−0.2953	−0.2917
2*p*	−127.1187	−127.0986	−127.2137	−462.3847	−462.2013	−464.2292
3*p*	−22.3445	−22.3736	−22.3896	−107.5593	−107.4376	−107.7708
4*p*	−2.7049	−2.7441	−2.7465	−22.1610	−22.1773	−22.2917
5*p*				−2.6781	−2.7646	−2.7691
3*d*	−14.4300	−14.4784	−14.4793	−83.6981	−84.3164	−84.0260
4*d*	−0.4784	−0.5112	−0.5113	−13.2774	−13.3317	−13.4501
5*d*				−0.3777	−0.4506	−0.4547
				−3.6059	−3.7448	−3.7838
Total atomic energy (hartree)	−5,314.69	−5,311.59	−5,310.66	−19,071.54	−18,986.88	−19,011.30
Ionization potential (eV)	6.07	6.29[c]	−5,314.51[d] 6.34[c]	7.48		−19,036.70[d]

[a] DKH results [9, 10]
[b] Numeric DHF results [28] unless noted otherwise. *p*-, *d*-, and *f*-orbital energies are averaged over spin–orbit components
[c] From Ref. [9]
[d] Finite-basis set DHF results from Ref. [14]

Au are in reasonable agreement with numeric DHF results. Because the basis sets employed are of moderate size, the valence orbital energies are affected by the incompleteness of the basis sets in the valence region. Thus, an extension of the basis sets by three even-tempered diffuse d-type functions leads to 5*d* orbital energies of −0.5097 hartree for Ag and of −0.4443 hartree for Au, which are considerably improved relative to the orbital energies reported in Table 3. The corresponding total energy is lowered by just 0.03 hartree for Ag and by 0.08 hartree for Au.

The quasi-relativistic method developed in the present work is based on a LO approximation to the exact relativistic Hamiltonian. An argument in favor of the present method is that it is variationally stable (which is not true for the Pauli approximation) and, accordingly, can be used within a quasi-variational procedure for obtaining the relativistic energy and wavefunction. This simplifies considerably the calculation of molecular geometries, frequencies, and other properties, in particular when they can be expressed as expectation values. Any perturbational approach is far less efficient in this respect as it has to revert to the calculation of response properties.

The proposed method, which is dubbed the LO-NESC-EP, performs better than the Pauli approximation. This is documented by the data in Tables 4 and 5. There, relativistic energy corrections to absolute and relative molecular energies as obtained with Eqs. (22), (23), and (24) within the HF approximation for a number of molecules containing first- and second-row elements are compared with the corresponding DHF values. Tarczay et al. [30] studied the same molecules within the Pauli approximation including either just one-electron (MVD1) or, alternatively, one- and two-electron terms (MVD2). Since the molecules studied (Tables 4, 5) contain only light elements, a comparison with the results from the perturbational approaches MVD1 and MVD2 is justified.

Figure 4 gives a graphical analysis of the calculated deviations from the DHF data [30] with regard to absolute relativistic corrections (Fig. 4a, Table 4) and with regard to the calculated energy barriers to rotation (C_2H_6), linearity (H_2O, H_2S, HNCO), inversion (NH_3, SiH_3^-, isomerization (HCN), and cyclization (SiC_2) (Fig. 4b, Table 5). The molecular structures and the results of the MVD1, MVD2, and DHF calculations were taken from Ref. [30]. The uncontracted cc-pCVDZ basis set [31] was used for the first-row elements and the uncontracted cc-pVDZ basis [31] augmented with tight d and f functions as suggested in Ref. [30] was employed for the second-row elements.

Figure 4 reveals that the LO-NESC-EP relative to MVD1 reduces the relative error in the relativistic energy corrections more than twice, both for absolute energies [average relative errors: 2.8% (LO-NESC-EP), 6.1% (MVD1), and 0.3% (MVD2)] and for reaction barriers [average relative errors: 5.2% (LO-NESC-EP), 12.1% (MVD1), and 7.2% (MVD2)]. Because the use of Eqs. (22), (23), and (24) just requires the inclusion of one-electron relativistic terms, an improvement relative to the traditional one-electron approximation is obvious. Although the LO-NESC-EP relativistic corrections to the total molecular energy are inferior to MVD2, the energy differences (reaction barriers) are of essentially the same quality as from MVD2; thus, the missing two-electron terms do not affect the chemically relevant properties as obtained with the use of Eqs. (22), (23), and (24). It should be noted, however, that the magnitude of the two-electron relativistic terms neglected in Eqs. (22), (23), and (24) is not identical to the difference MVD2−MVD1. The results in Table 2 suggest that for light elements the energetic effect of the neglected two-electron terms is about 30% smaller than the magnitude of the two-electron Darwin correction [30].

Table 4. Relativistic energy corrections (mhartree) to total energies of selected molecules as obtained at the Hartree–Fock level of theory. The molecular structures are taken from Ref. [30]. The uncontracted cc-pCVDZ basis set is used for first-row elements and the uncontracted cc-pVDZ basis modified as described in Ref. [30] for Si and S

Molecule	This work	MVD1[b]	MVD2[c]	DHF[d]
C_2H_6	−30.397	−29.175	−31.831	−31.853
NH_3	−29.772	−28.697	−30.895	−30.926
H_2O	−53.281	−51.499	−54.902	−54.980
HCN	−45.333	−43.634	−47.158	−47.200
HNCO	−98.529	−95.039	−101.955	−102.074
SiH_3^-	−616.46	−599.72	−621.60	−624.59
SiC_2	−647.92	−629.42	−645.46	−657.48
H_2S	−1,104.71	−1,075.44	−1,109.55	−1,116.56

[a] Sum of one-electron mass-velocity and Darwin corrections as calculated in Ref. [30]
[b] Sum of one-electron mass-velocity and one- and two-electron Darwin corrections as calculated in Ref. [30]
[c] DHF energies as calculated in Ref. [30]

Table 5. Relativistic energy corrections (cm^{-1}) to barriers of selected molecules as obtained at the Hartree–Fock level of theory. See legend to Table 4

Molecule	This work	MVD1	MVD2	DHF
C_2H_6[a]	0.58	0.52	0.58	0.57
NH_3[b]	23.64	22.98	24.21	24.26
H_2O[c]	60.92	59.50	62.32	62.50
HCN[d]	15.69	15.36	15.78	15.69
N···H···C[e]	−32.68	−31.41	−33.10	−33.31
HNCO[f]	33.00	31.95	33.69	33.85
$SiH3_b^-$	106.3	102.9	105.6	104.5
SiC_2[g]	−2.1	−1.0	−1.2	−3.5
H_2S[c]	233.3	227.3	232.6	234.8

[a] Barrier to rotation
[b] Barrier to inversion
[c] Barrier to linearity
[d] HCN–HNC isomerization energy
[e] Barrier to HCN–HNC isomerization
[f] Barrier to cis–trans isomerization
[g] Energy difference between linear Si−C−C and the triangular form

4 Conclusions

In this work we have shown that by a slight modification, the LO-NESC (NESC $\mathbf{U}=\mathbf{I}$) [19] can be converted into a variationally stable method. The modification is

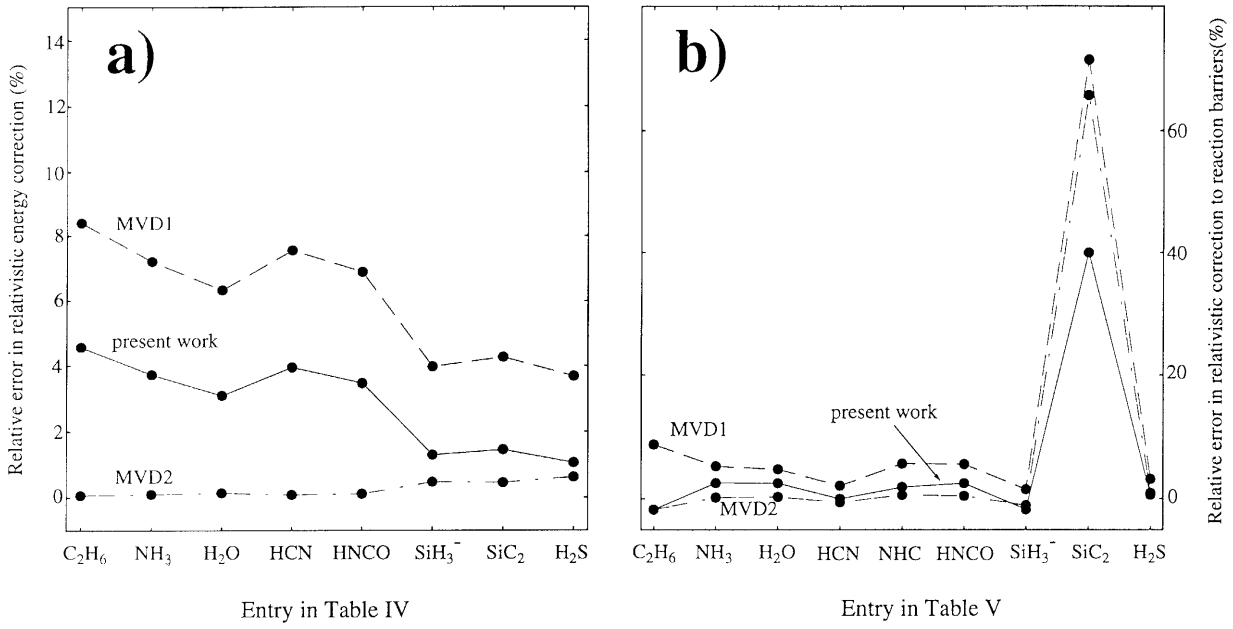

Fig. 4. Relative percentage error in the calculated relativistic corrections **a** to the total energy and **b** to the reaction barriers for selected molecular systems. See text and Tables 4 and 5 for more details

physically motivated and involves the use of a cutoff factor in the relativistic correction to the nuclear–electron attraction term. As shown in Sect. 2, the relativistic correction to the nuclear attraction potential behaves regularly near the nucleus in case of the exact NESC [15] scheme. In the approximate scheme proposed here, this effect is modeled by an energy-independent cutoff factor which regularizes the bare nuclear potential at distances shorter than $r \sim Z/(mc^2)$. The LO-NESC-EP approach possesses the following advantages:

1. The LO-NESC-EP is variationally stable. This is verified by a theoretical analysis in Sect. 2 and the Appendix and by numeric results in Sects. 2 and 3.
2. The LO-NESC-EP employs the energy-independent quasi-relativistic metric which simplifies considerably the calculation of the two-electron terms in the Hamiltonian.
3. The LO-NESC-EP provides an accurate description of the relativistic correction to the total energy for atomic and molecular systems as exemplified by the numeric results for hydrogen-like and helium-like atomic ions with Z up to 100, the results for Ag and Au atoms in their ground states, and the results of molecular calculations (see also Ref. [32]).
4. The Hamiltonian operator of the LO-NESC-EP does not contain any unusual terms which do not appear in the nonrelativistic Hamiltonian. All integrals in the LO-NESC-EP Hamiltonian matrix can be evaluated analytically using the existing nonrelativistic software.

Because of the latter feature, the LO-NESC-EP can be easily installed within any existing nonrelativistic quantum-chemical computer program. In this respect, it represents a useful starting basis for the ultimate goal of our research, namely

1. Setting up the LO-NESC-EP for density functional theory (DFT) to calculate molecular energies for larger molecular systems [32].
2. Developing for the resulting DFT method analytical energy gradients to calculate routinely molecular geometries.
3. Adding the spin–orbit coupling correction to the quasi-relativistic corrections described in this work.
4. Extending the DFT LO-NESC-EP for the calculation of relativistically corrected NMR chemical shifts.
5. Merging the approach with empirical methods within a generally applicable quantum mechanical/molecular mechanics program.

Although a genuine relativistic method will guarantee higher accuracy, the present method seems to us better suited to investigate the potential-energy surfaces, thermodynamic properties, and spectroscopic characteristics of large molecular systems containing heavy atoms, in particular those of biochemical interest. Although some of these goals are feasible within the effective core potential approach [33], the calculation of magnetic properties that depend on the core electrons can only be carried out if relativistic corrections are explicitly considered in the all-electron Hamiltonian. The application of the LO-NESC-EP to molecular calculations is considered elsewhere [32].

Acknowledgements. This work was supported at Göteborg by the Swedish Natural Science Research Council. Calculations were done on the supercomputers of the Nationellt Superdatorcentrum, Linköping, Sweden.

Appendix

The potential of a uniformly charged sphere of radius r_0 is given by Eq. (A1):

$$V'_{\mathrm{ne}}(\mathbf{r}) = \begin{cases} -\frac{Z}{2r_0}\left[3 - \left(\frac{r}{r_0}\right)^2\right] & r \le r_0 \\ -\frac{Z}{r} & r > r_0 \end{cases} \tag{A1}$$

Using Eq. (A1) the expectation value of the Hamiltonian (Eq. 15) can be expressed as

$$\begin{aligned}\langle \hat{H} \rangle &= \left\langle \Phi \middle| T + V_{\mathrm{ne}} + \frac{1}{4m^2c^2}(\sigma\cdot\mathbf{p})V'_{\mathrm{ne}}(\sigma\cdot\mathbf{p}) \middle| \Phi \right\rangle \\ &= \left\langle (\sigma\cdot\mathbf{p})\Phi \middle| \frac{1}{2m} + \frac{1}{4m^2c^2}V'_{\mathrm{ne}} \middle| (\sigma\cdot\mathbf{p})\Phi \right\rangle + \langle \Phi | V_{ne} | \Phi \rangle \ ,\end{aligned} \tag{A2}$$

where the hermiticity of the kinetic energy operator (Eq. 46) and the $\sigma\cdot\mathbf{p}$ operator was used. Substituting Eq. (A1) into Eq. (A2) one obtains

$$\begin{aligned}\langle \hat{H} \rangle = &\int_{r\le r_0} |(\sigma\cdot\mathbf{p})\Phi|^2 \left(\frac{1}{2m} - \frac{3Z}{8m^2c^2}\frac{1}{r_0}\right) d\mathbf{r} + \int_{r\le r_0} |\Phi|^2 V_{\mathrm{ne}} \mathrm{d}\mathbf{r} \\ &+ \int_{r\le r_0} |(\sigma\cdot\mathbf{p})\Phi|^2 \frac{Z}{8m^2c^2}\frac{r^2}{r_0^3} \mathrm{d}\mathbf{r} \\ &+ \int_{r>r_0} |(\sigma\cdot\mathbf{p})\Phi|^2 \left(\frac{1}{2m} - \frac{1}{4m^2c^2}\frac{Z}{r}\right) \mathrm{d}\mathbf{r} \\ &+ \int_{r>r_0} |\Phi|^2 V_{\mathrm{ne}} \mathrm{d}\mathbf{r}.\end{aligned} \tag{A3}$$

The integration limits $r \le r_0$ and $r > r_0$ indicate whether the integration is performed within the sphere of radius r_0 or outside the sphere, respectively.

Provided that a trial function Φ falls off exponentially as $r\to\infty$, integration outside the sphere leads to a finite value. As for the three integrations inside the sphere (first, second, and third term on the rhs of Eq. A3), only the first and the second integrals can adopt negative values. The second integral is always negative as it represents the potential-energy contribution, while the first integral will become negative if the term in parentheses is negative. With nonsingular trial function, for example, of Gaussian or Slater type, the first integral in Eq. (A3) is proportional to the square of an exponential parameter; hence, this integral can be made infinitely negative with an appropriate choice of the exponential parameter provided that the term in parentheses is negative. If the trial function is singular, for example, of type expressed in Eq. (20), the integrand in the first integral in Eq. (A3) is more singular than the integrand in the second term. Thus, this integral will diverge faster than the potential-energy contribution as the trial function will become more and more singular. Consequently, in order to guarantee the lower bound for the Hamiltonian expectation value $\langle \hat{H} \rangle$, the integrand in the first integral in Eq. (A3) must always be positive. This leads to Eq. (A4) for the cutoff radius, r_0:

$$r_0 > \frac{3}{4}\frac{Z}{mc^2} \ . \tag{A4}$$

Provided the cutoff radius fulfills this condition, the expectation value of the quasi-relativistic Hamiltonian with the potential in Eq. (A1) is limited from below.

If the potential in Eq. (14) of a Gaussian charge distribution is used for V'_{ne}, the limiting value of the cutoff radius, which provides a lower bound for $\langle \hat{H} \rangle$, can be obtained from Eq. (A4) considering that in the vicinity of the nucleus the potential in Eq. (14) behaves approximately as in Eq. (A5):

$$V(r \to 0) \approx -\frac{2}{\sqrt{\pi}}\frac{Z}{r_0}\left[1 - \frac{1}{3}\left(\frac{r}{r_0}\right)^2\right] . \tag{A5}$$

By using Eq. (A5) instead of Eq. (A1) in the first term in Eq.(A3), Eq. (A6) is obtained,

$$r_0 > \frac{1}{\sqrt{\pi}}\frac{Z}{mc^2} \ , \tag{A6}$$

which guarantees the existence of a lower bound of the Hamiltonian in Eq. (15). The essence of Eqs. (A4) and (A6) can be given by Eq. (A7):

$$V'_{\mathrm{ne}}(0) > -2mc^2 \ . \tag{A7}$$

It is interesting to note that Eq. (A7) guarantees positive definiteness of the total energy defined by Eq. (15) when the orbital exponent ζ in Eq. (20) approaches infinity. This conclusion can be inferred from the scaling transformation $\mathbf{r}\to\lambda\mathbf{r}$ applied to the energy expectation value, which yields the energy as a function of the scaling parameter λ:

$$E(\lambda) = \frac{\lambda^2\left\langle (\sigma\cdot\mathbf{p})\Phi \middle| \frac{1}{2m} + \frac{1}{4m^2c^2}V'_{\mathrm{ne}}(r/\lambda) \middle| (\sigma\cdot\mathbf{p})\Phi \right\rangle + \langle \Phi | V_{\mathrm{ne}}(r/\lambda) | \Phi \rangle}{\langle \Phi | \Phi \rangle + \lambda^2 \left\langle (\sigma\cdot\mathbf{p})\Phi \middle| \frac{1}{4m^2c^2} \middle| (\sigma\cdot\mathbf{p})\Phi \right\rangle} \ . \tag{A8}$$

As the coordinate scaling parameter λ approaches infinity, the trial wavefunction (Eq. 20) collapses towards the nucleus. Requiring the positive definiteness of $E(\lambda\to\infty)$ yields Eq. (A7) for an admissible potential V'_{ne}. This conclusion is supported by the asymptotic behavior of the energy expectation value calculated with the trial function in Eq. (20). Using the potential in Eq. (A1) with the cutoff radius from Eq. (19) one has $\lim_{\zeta\to\infty} E = \frac{1}{2}mc^2$.

References

1. (a) Pyykkö P (1988) Chem Rev 88:563; (b) Pyykkö P (1997) Chem Rev 97: 597
2. Schwarz WHE (1990) In: Maksi ZB (ed) Theoretical models of chemical bonding. Part 2. The concept of the chemical bond. Springer, Berlin Heidelberg New York, p 593
3. Almlöf J, Gropen O (1996) In: Lipkowitz KB, Boyd DB (eds) Reviews in computational chemistry, vol. 8. VCH, New York, p 203
4. Swirles B (1935) Proc R Soc Lond Ser A 152: 625
5. Sucher J (1980) Phys Rev A 22: 348
6. Quiney HM, Skaane H, Grant IP (1999) Adv Quantum Chem 32: 1

7. Foldy LL, Wouthuysen SA (1950) Phys Rev 78: 29
8. Douglas M, Kroll NM (1974) Ann Phys NY 82: 89
9. (a) Hess BA (1985) Phys Rev A 32:756; (b) Hess BA (1986) Phys Rev A 33: 3742
10. Samzow R, Hess BA, Jansen G (1992) J Chem Phys 96: 1227
11. (a) Chang C, Pelissier M, Durand P (1986) Phys Scr 34: 394; (b) Heully J-L, Lindgren I, Lindroth E, Lundqvist S, Mårtenson-Pendrill A-M (1986) J Phys B 19: 2799
12. van Leeuwen R, van Lenthe E, Baerends EJ, Snijders JG (1994) J Chem Phys 101: 1272
13. van Lenthe E, Baerends EJ, Snijders JG (1994) J Chem Phys 101: 9783
14. Nakajima T, Hirao K (1999) Chem Phys Lett 302: 383
15. Dyall KG (1997) J Chem Phys 106: 9618
16. (a) Sewell GL (1949) Proc Camb Philos Soc 45: 631; (b) Rutkowski A (1986) J Phys B 19: 149; (c) Rutkowski A (1986) J Phys B 19: 3431; (d) Rutkowski A (1986) J Phys B 19: 3443; (e) Rutkowski A, Jankowski K, Mikielewicz B (1988) J Phys B 21: L147; (f) Rutkowski A, Rutkowska D, Schwarz WHE (1992) Theor Chim Acta 84: 105; (g) Kutzelnigg W (1989) Z Phys D 11: 15; (h) Kutzelnigg W (1990) Z Phys D 15: 27; (i) Kutzelnigg W (1996) Phys Rev A 54: 1183
17. van Wüllen C (1998) J Chem Phys 109: 392
18. Barysz M (2000) J Chem Phys 113: 4003
19. Dyall KG (1998) J Chem Phys 109: 4201
20. Dirac PAM (1928) Proc R Soc Lond A 117: 610
21. Pauli W (1927) Z Phys 43: 601
22. Dyall KG (1994) J Chem Phys 100: 2118
23. Visser O, Aerts PJC, Hegarty D, Nieuwpoort WC (1987) Chem Phys Lett 134: 34
24. (a) Velde GT, Bickelhaupt FM, Baerends EJ, Guerra CF, van Gisbergen SJA, Snijders JG, Ziegler T (2001) J Comput Chem 22: 931; (b) Belanzoni P, van Lenthe E, Baerends EJ (2001) J Chem Phys 114: 442; (c) Stein M, van Lenthe E, Baerends EJ, Lubitz W (2001) J Phys Chem A 105: 416; (d) Hong GY, Dolg M, Li LM (2000) Int J Quantum Chem 80: 201; (e) van Lenthe E, Baerends EJ (2000) J Chem Phys 112: 8279; (f) Bouten R, Baerends EJ, van Lenthe E, Visscher L, Schreckenbach G, Ziegler T (2000) J Phys Chem A 104: 5600; (g) van Lenthe E, Ehlers A, Baerends EJ (1999) J Chem Phys 110: 8943; (h) van Lenthe E, van der Avoird A, Wormer PES (1998) J Chem Phys 108: 4783; (i) van Lenthe E, Wormer PES, van der Avoird A (1997) J Chem Phys 107: 2488; (j) van Lenthe E, Snijders JG, Baerends EJ (1996) J Chem Phys 105: 6505
25. Goldman SP (1988) Phys Rev A 37: 16
26. Ishikawa Y, Quiney HM (1993) Phys Rev A 47: 1732
27. Indelicato P (1995) Phys Rev A 51: 1132
28. Desclaux JP (1973) At Data Nucl Data Tables 12: 311
29. Gropen O (1987) J Comput Chem 8: 982
30. Tarczay G, Csäszär A, Klopper W, Quiney HM (2001) Mol Phys 99: 1769
31. (a) Woon D, Dunning TH Jr (1995) J Chem Phys 103: 4572; (b) Woon DE, Dunning TH Jr (1993) J Chem Phys 98: 1358
32. Filatov M, Cremer D (2002) Chem Phys Lett 351: 259
33. (a) Dolg M (2000) In: Grotendorst J (ed) Modern methods and algorithms of quantum chemistry. Proceedings, 2nd edn, vol 3. John von Neumann Institute for Computing, Jülich, p 507; (b) Dyall KG (2001) J Chem Inf Comput Sci 41: 30